

Investigating the role of microbubbles and focused ultrasound in tissue temperature elevation

¹Diego Vaca-Revelo; ²Kaleb Vuong; ²Michalakis Averkiou; ¹Aswin Gnanaskandan*

¹*Worcester Polytechnic Institute, USA*

²*University of Washington, Seattle, USA*

Abstract.

The objective of this study is to elucidate the ‘acoustic to thermal energy conversion’ mechanisms in microbubble assisted high intensity focused ultrasound (HIFU) therapy. HIFU uses high intensity ultrasound (US) to elevate the temperature of a biological medium. It has been suggested that introducing encapsulated microbubbles in the target region increases heat deposition in that region even at lower acoustic pressure, thus preventing any unwanted damage due to high acoustic pressure source. However, the exact mechanism through which microbubbles enhance heat deposition is still unclear. We use numerical simulations validated with laboratory experiments to investigate the physics of microbubble-assisted temperature elevation in HIFU. The experiments are conducted on a gel phantom infused with microbubbles and insonated with a single element transducer. Both temperature and pressure are measured in real time. The ultrasound field is modelled using compressible Navier-Stokes equations on a fixed grid and the bubbles are represented in a Lagrangian framework. The coupling of the frameworks is achieved through a local volume averaging. The experiments allow us to study the acoustic and thermal fields at a macroscopic level. These results are then used to develop and validate the multiscale CFD model which facilitates parametric studies of key variables across a wide range of therapeutically relevant conditions. The combined experiments and simulations will be used to elucidate the mechanisms by which microbubbles enhance the acoustic to thermal energy conversion process.

Introduction

High-Intensity Focused Ultrasound (HIFU) therapy is a medical procedure that has been approved by the U.S. Food and Drug Administration for treating uterine fibroids and subsurface prostate cancer. The fundamental concept behind HIFU involves converting acoustic energy into thermal energy by focusing the ultrasound waves (US) onto the target area. The thermoviscous absorption of the sound waves results in a temperature increase mainly in the focal region of the HIFU beam. The importance of HIFU therapy lies in its non-invasive nature and it has the potential to treat deep-seated cancers like those in the liver and brain. However, treating deeper targets requires a higher acoustic intensity source, increasing the risk of harming adjacent healthy tissue. Hence it is desirable to achieve high focal temperature elevation while using moderate source intensity levels. Various techniques have been proposed to achieve this while minimizing surrounding tissue damage. These include including incorporating cooling periods between heating cycles, prolonging the medical procedure, and introducing encapsulated microbubbles as contrast agents [1], [2]. Among these, introducing encapsulated microbubbles to enhance heat deposition is considered promising and has been explored both experimentally [3], [4] and numerically [5], [6]. However, the exact physical mechanisms through which microbubbles enhance the heat depositions is not elucidated clearly yet.

Ultrasound-initiated microbubble oscillations can modify the local pressure and acoustic streaming velocity in the medium, both of which contribute to a more efficient energy conversion from acoustic to thermal mode. The bubbles can modify the local pressure, streaming velocity, and as a result the temperature field, through three major mechanisms: acoustic damping, viscous damping, and thermal damping of bubble oscillations [7]. Acoustic damping of bubble oscillations results from the emission of acoustic energy by the bubble. Viscous damping occurs due to viscous dissipation of energy in the relatively thin viscous layer of the host medium surrounding the bubble during its oscillations. Finally, thermal damping is associated with the thermodynamics of an oscillating bubble, where thermal energy enters the bubble during its expansion phase and exits during its collapse phase. It is unknown what

relative roles each of the mechanisms discussed above play in microbubble enhanced HIFU, the knowledge of which is essential to control and maximize the thermal ablation of targeted tissues. Further, accurate characterization of the acoustic and thermal fields generated by mb-HIFU at different points on the targeted and neighboring tissues remains undone due to the difficulty in experimental characterization of such a nonlinear bubble-acoustics-thermal field interaction phenomenon. The main aim of this work is to develop a numerical method to simulate microbubble enhanced HIFU and validate it using novel *in vitro* experiments to answer the above questions.

Physical model and numerical method

The numerical method we develop is based on a Eulerian-Lagrangian approach in which the nonlinear ultrasound propagation is computed using a fixed grid Eulerian approach, while the location and size of the individual microbubbles are tracked in a Lagrangian framework. These two frameworks are coupled to each other such that there is a two-way interaction between them. In the Eulerian framework, we solve the compressible Navier Stokes equations and the advection equations of the volume fraction of each species in a fixed grid; the system of equations is closed using the stiffened-gas equation of state. A 4th order Runge Kutta method, HLLC Riemann solver and a WENO based reconstruction are used to solve the governing equations. For more details on the equations, numerical method and validation please refer to Bryngelson et al. [8]. For the Lagrangian framework we solve the bubble dynamics described by Keller-Miksis equation. The insonation time during clinical operation is of the order of one second. This is 10^6 times the period of the acoustic waves. Since the time accurate acoustic field computations are limited to hundreds of cycles only, we use a decoupled approach for heat transfer solver, where we first develop the flow field using the Eulerian-Lagrangian approach. Time averaged heat deposition terms are then derived from the obtained bubble-acoustic field and are used as heat source terms to solve a bio heat transfer equation, which addresses the longer time.

Experimental setup

The experimental setup shown in Figure 1 has a tissue phantom or water insonified from the side with a single element focused transducer. Ultrasound pulses are generated with an arbitrary function generator and amplified by a power amplifier. The thermocouple is positioned in the phantom such that its tip is exactly at the focus of the HIFU transducer to take temperature measurements. Alignment of the HIFU transducer and the needle thermocouple is done with the help of ultrasound imaging and with the method described previously in [9].

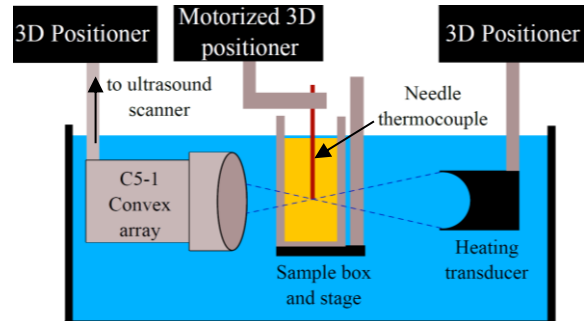


Figure 1: Schematic of the experimental set up.

Results and discussion

Validation of the Eulerian framework solver

The Eulerian framework solver is validated by conducting HIFU simulation in water in both linear and non-linear wave propagation regimes. For the linear regime, a 1.074 MHz hemispherical transducer of diameter 41.5 mm and focal length 44.5 mm generates acoustic waves of amplitude 0.029 MPa within a water tank. Figure 2 illustrates the focal scan comparison of the peak-to-peak pressure profiles along the axisymmetric and transverse axes. The numerical results closely align with our experimental findings, effectively capturing the focused ultrasound area and corresponding focal pressure. For the non-linear regime, we compare our simulations with the experiments reported by Canney et al. [10] in water; their setup involves a 2.158 MHz transducer (diameter: 42.0 mm and focal length: 44.4 mm) to produce sound waves with an amplitude of 0.29 MPa. We simulated this configuration with two different grid sizes; the coarse grid resolved the wavelength using 35 grid points and the fine grid using 70 grid points. The simulation with the fine grid reproduces better the pressure peaks over time which is shown in Figure 3, but it approximately doubled the computational time needed.

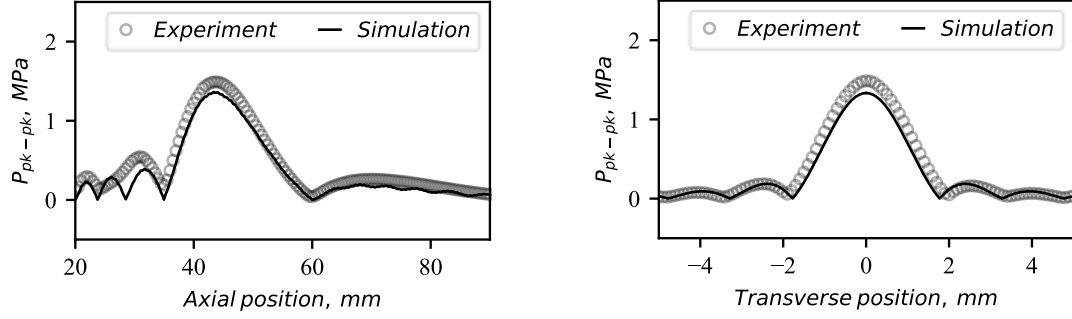


Figure 2: Peak-to-peak focal scans along the axisymmetric (a) and transverse (b) axes in the linear regime.

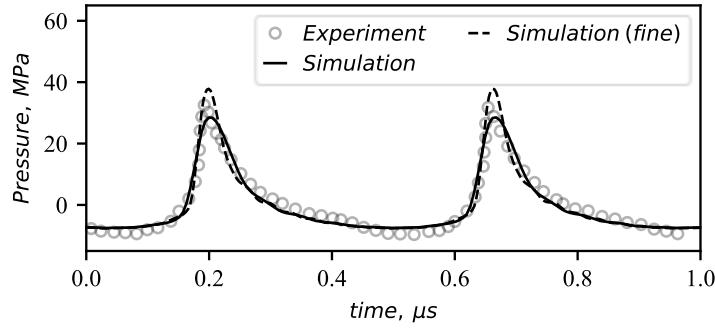


Figure 3: Pressure evolution at the focus in the non-linear regime; the experimental data were taken from [10].

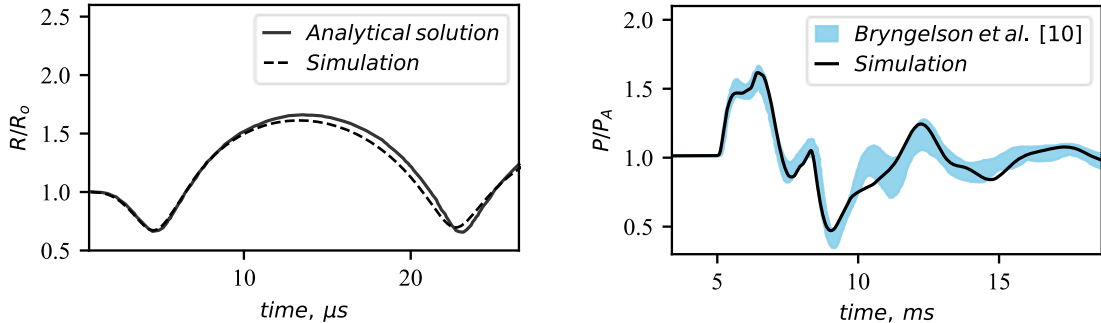


Figure 4: (a) Evolution of a single, isolated bubble, and (b) pressure evolution at the center of a bubble cloud under excitation by a single cycle of a sinusoidal pressure wave.

Validation of the Lagrangian framework solver

The accuracy of the Lagrangian framework solver is thoroughly examined through two distinct simulations designed to predict the dynamic behavior of bubbles under specific conditions. In the first simulation, an isolated bubble of 50 μm diameter with fixed location encounters a single sinusoidal acoustic wave of 0.2 MPa of amplitude, and 150 kHz of frequency. The resulting evolution of the bubble's radius, as illustrated in Figure 4a, is compared with the analytical solution of the Keller–Miksis equation showing good agreement. For the next simulation, a single sinusoidal pressure wave (0.1 MPa of amplitude and 300 kHz of frequency) interacts with a monodisperse cloud of bubbles initially of diameter 10 μm contained within a 5mm cubic space. The blue region in Figure 4b shows the pressure evolution at the cloud center for various simulations with different bubble spatial distribution reported by Bryngelson et al. [11]. Our pressure evolution curve predominantly resides within this region assuring

that our solver captures well not only the behavior of a single bubble, but also the dynamics of a cloud of bubbles.

Simulation of HIFU wave propagation and heat deposition in a tissue phantom

Having gained confidence in the validity of the solver, we proceed to simulate the heat deposition due to focused US propagation in a tissue like medium. An egg white phantom is used since its properties are close to those of tissue. The acoustic properties of the egg white phantom, experimentally measured, include a density of 1040 kg/m^3 , speed of sound at 1580 m/s , and an attenuation coefficient of 0.29 dB/cm MHz ($\mu=0.0878 \text{ Pa.s}$). Its thermodynamic properties are assumed to be $K = 0.59 \text{ W/mK}$ and $Cp = 4270 \text{ J/kg K}$ [12]. Here, HIFU propagates in water for 19.5 mm and then propagates in the egg white medium reaching the focal point at 44.5 mm from the transducer. The 1.074 MHz hemispherical transducer has an aperture diameter of 41.5 mm and generates sound waves with a source amplitude of 0.029 MPa for study case A, and 0.058 MPa for case B. Figure 5a illustrates the instantaneous pressure field where the maximum pressure is reached at the geometric focal point. The instantaneous heat source (q_{US}) is computed from the acoustic field, quantifying the heat absorbed by the phantom tissue. Then, this heat source is averaged over $30\mu\text{s}$, equivalent to 32 sinusoidal wave cycles. Figure 5b illustrates the logarithm of the time-averaged q_{US} showing the maximum values in the geometric focus and minimum values in the pre and post-focal regions. The ultrasound source is activated for 30 seconds, followed by a 30 -second cooling period. Examining the instantaneous temperature field in Figure 6a, it is evident that the highest temperature is reached in the focal region. The numerical temperature profiles agree well with the experimental profiles in cases A and B, as verified in Figure 6b. Thus, the numerical methodology predicts well the acoustic to thermal energy conversion of focused ultrasound waves propagating in a medium without bubbles.

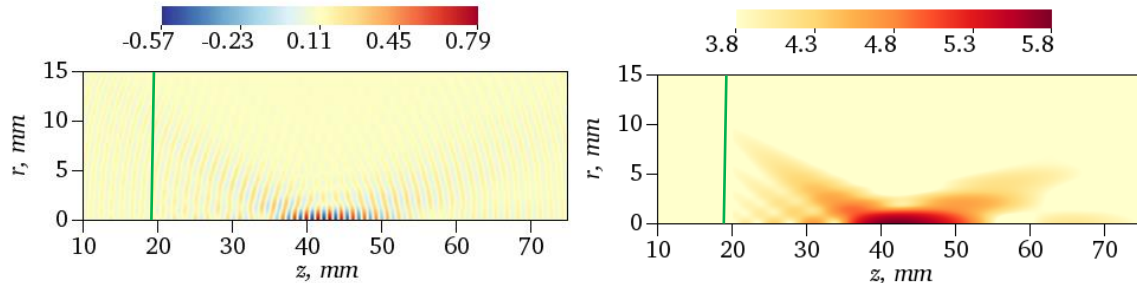


Figure 5: (a) Instantaneous contours of the pressure field, MPa and (b) contours of the logarithm of time-averaged heat source, $\log (\text{J/m}^3\text{s})$ over $30 \mu\text{s}$ for case A. The green line shows the water-phantom interface.

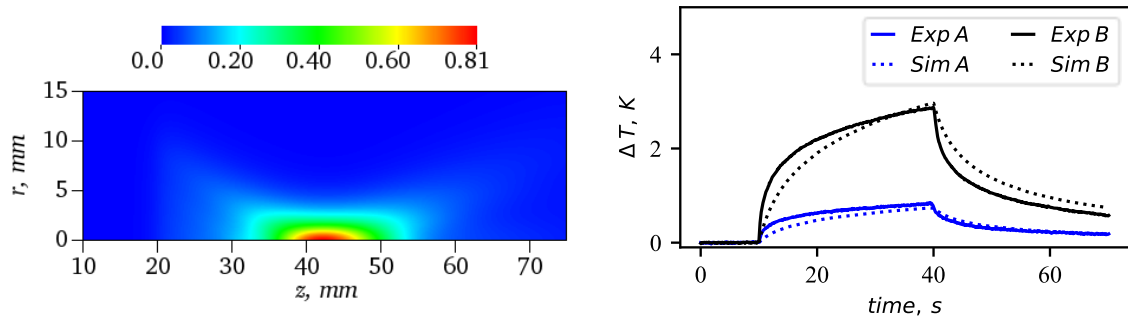


Figure 6: (a) Instantaneous temperature field, K, after 30 sec of insonation for case A, and (b) comparison of the experimental and simulated temperature evolution profiles in the focal region for cases A and B.

Summary

A Euler-Lagrange method is developed to study the heat deposition due to microbubbles and focused ultrasound in a tissue-like medium. The model is validated using experiments conducted in water and egg white phantom demonstrating very good agreement for both pressure and thermal fields. The next

step is to study the heat deposition due to acoustic, viscous, and thermal damping of microbubbles and validate using *in vitro* experiments. Ultimately, our aim is to elucidate a better understanding of the role of microbubbles in tissue temperature elevation.

Acknowledgments

We gratefully acknowledge the support from the U. S. National Science Foundation (NSF) under the grants CBET 2301721 and CBET 2301709.

References

- [1] Y. Kaneko *et al.*, “Use of a microbubble agent to increase the effects of high intensity focused ultrasound on liver tissue,” *Eur Radiol*, vol. 15, no. 7, pp. 1415–1420, Jul. 2005, doi: 10.1007/S00330-005-2663-7.
- [2] D. J. Chung, S. H. Cho, J. M. Lee, and S. T. Hahn, “Effect of microbubble contrast agent during high intensity focused ultrasound ablation on rabbit liver *in vivo*,” *Eur J Radiol*, vol. 81, no. 4, pp. e519–e523, Apr. 2012, doi: 10.1016/J.EJRAD.2011.06.002.
- [3] A. Clark, S. Bonilla, D. Suo, Y. Shapira, and M. Averkiou, “Microbubble-Enhanced Heating: Exploring the Effect of Microbubble Concentration and Pressure Amplitude on High-Intensity Focused Ultrasound Treatments,” *Ultrasound Med Biol*, vol. 47, no. 8, pp. 2296–2309, Aug. 2021, doi: 10.1016/J.ULTRASMEDBIO.2021.03.035.
- [4] E. K. Juang, L. H. De Koninck, K. S. Vuong, A. Gnanaskandan, C. T. Hsiao, and M. A. Averkiou, “Controlled Hyperthermia With High-Intensity Focused Ultrasound and Ultrasound Contrast Agent Microbubbles in Porcine Liver,” *Ultrasound Med Biol*, vol. 49, no. 8, pp. 1852–1860, Aug. 2023, doi: 10.1016/J.ULTRASMEDBIO.2023.04.015.
- [5] A. Gnanaskandan, C. T. Hsiao, and G. Chahine, “Modeling of Microbubble-Enhanced High-Intensity Focused Ultrasound,” *Ultrasound Med Biol*, vol. 45, no. 7, pp. 1743–1761, Jul. 2019, doi: 10.1016/J.ULTRASMEDBIO.2019.02.022.
- [6] A. Gnanaskandan, C.-T. Hsiao, and G. Chahine, “Contrast agent shell properties effects on heat deposition in bubble enhanced high intensity focused ultrasound,” *J Acoust Soc Am*, vol. 149, no. 1, pp. 421–434, Jan. 2021, doi: 10.1121/10.0002948.
- [7] C. Barajas and E. Johnsen, “The effects of heat and mass diffusion on freely oscillating bubbles in a viscoelastic, tissue-like medium,” *J Acoust Soc Am*, vol. 141, no. 2, pp. 908–918, Feb. 2017, doi: 10.1121/1.4976081.
- [8] S. H. Bryngelson, K. Schmidmayer, V. Coralic, J. C. Meng, K. Maeda, and T. Colonius, “MFC: An open-source high-order multi-component, multi-phase, and multi-scale compressible flow solver,” *Comput Phys Commun*, vol. 266, p. 107396, Sep. 2021, doi: 10.1016/J.CPC.2020.107396.
- [9] C. P. Keravnou, I. De Cock, I. Lentacker, M. L. Izamis, and M. A. Averkiou, “Microvascular Injury and Perfusion Changes Induced by Ultrasound and Microbubbles in a Machine-Perfused Pig Liver,” *Ultrasound Med Biol*, vol. 42, no. 11, pp. 2676–2686, Nov. 2016, doi: 10.1016/J.ULTRASMEDBIO.2016.06.025.
- [10] M. S. Canney, M. R. Bailey, L. A. Crum, V. A. Khokhlova, and O. A. Sapozhnikov, “Acoustic characterization of high intensity focused ultrasound fields: A combined measurement and modeling approach,” *J Acoust Soc Am*, vol. 124, no. 4, pp. 2406–2420, Oct. 2008, doi: 10.1121/1.2967836.
- [11] S. H. Bryngelson, K. Schmidmayer, and T. Colonius, “A quantitative comparison of phase-averaged models for bubbly, cavitating flows,” *International Journal of Multiphase Flow*, vol. 115, pp. 137–143, 2019, doi: 10.1016/j.ijmultiphaseflow.2019.03.028.
- [12] G. W. Divkovic, M. Liebler, K. Braun, T. Dreyer, P. E. Huber, and J. W. Jenne, “Thermal Properties and Changes of Acoustic Parameters in an Egg White Phantom During Heating and Coagulation by High Intensity Focused Ultrasound,” *Ultrasound Med Biol*, vol. 33, no. 6, pp. 981–986, Jun. 2007, doi: 10.1016/J.ULTRASMEDBIO.2006.11.021.